Scaling of the Droplet-Size Distribution in Vapor-Deposited Thin Films

Fereydoon Family(1) and Paul Meakin(2)
(1)*Department of Physics, Emory University, Atlanta, Georgia 30322*
(2)*Central Research and Development Department, E. I. DuPont de Nemours and Company, Wilmington, Delaware 91881*

(Received 26 April 1988)

A dynamic-scaling approach is developed for the description of the droplet-size distribution in vapor-deposited thin films and processes where droplets are formed by nucleation, growth, and coalescence of the droplets. The exponent describing the scaling of the droplet-size distribution and the growth law for the mean droplet size are calculated exactly. A realistic, yet simple, droplet-growth model is developed. The simulation data are found to be consistent with the experiments on vapor-deposited tin and with the theoretical predictions in $d=1$, 2, and 3.

PACS numbers: 64.60.Ak, 64.60.Qb, 68.45.Da, 82.60.Nh

Thin films are used in an ever increasing number of scientific and industrial applications. Understanding the kinetics of their formation is a challenging problem of considerable theoretical and experimental interest.[1] Frequently in thin-film deposition the initial layer condenses as discrete droplets, which grow and coalesce to form larger droplets, eventually forming a complete layer. This occurs[1] when the binding energy of the condensate atoms to each other is greater than their binding energy to the substrate. The most characteristic feature of this process is the formation of a distribution of droplets of varying sizes which evolves with time. Figure 1(a) is an electron micrograph of vapor-deposited tin on the surface of a sapphire sample held at 230°C and clearly shows the distribution of tin droplets that have been formed. The formation of a distribution of droplets is the central feature of a number of other kinetic processes[1-5] and understanding the kinetics of droplet-size distribution is a problem of general interest.

Recent investigations of the temporal evolution of the cluster-size distributions in gelation,[6] aggregation,[7] and coagulation with fragmentation[8] have advanced our understanding of the kinetics of a variety of growth phenomena.[9] A particularly significant outcome of these studies was the realization that the cluster-size distribution and its moments are scale invariant and the tech-

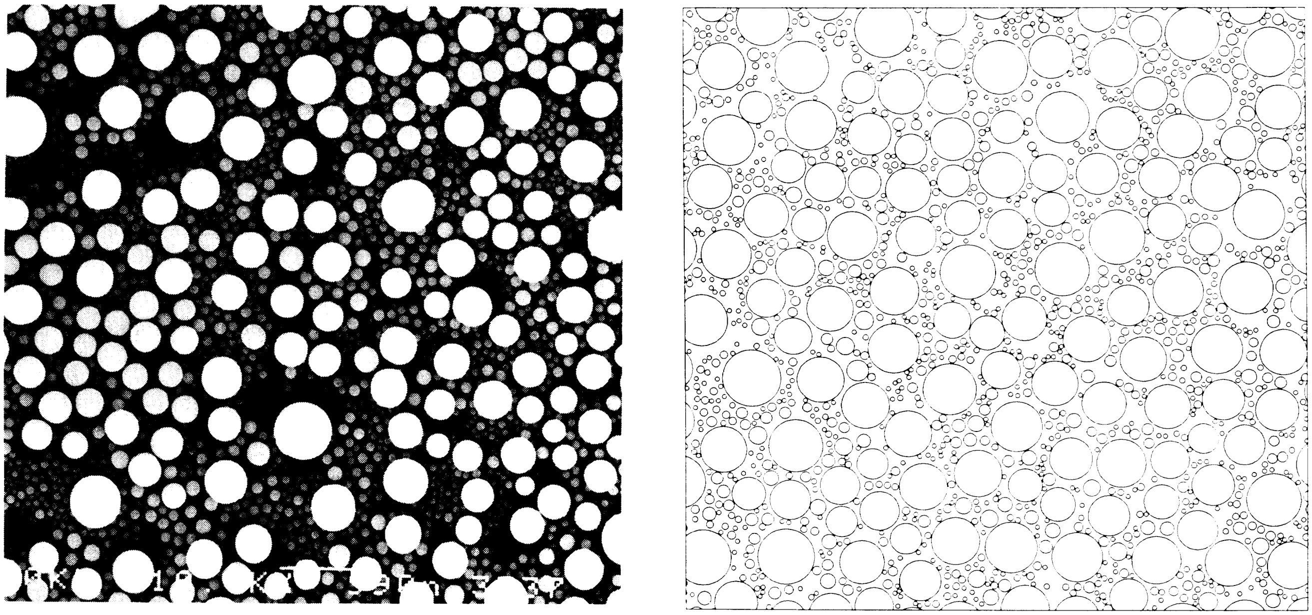
(a) (b)

FIG. 1. (a) An electron micrograph of vapor-deposited tin on the surface of a sapphire sample held at 230 °C. The uniform size of the larger droplets indicates that there exists an approximately monodispersed distribution of droplets which is superimposed on wide distribution of smaller droplets. (b) A typical example from the simulation in which spherical droplets with a radius $r_0=0.75$ were added at random to a surface of size 256×256. Depleted zones around large droplets are evident in both figures.

niques developed for understanding scaling phenomena could be applied to these systems.[7-9] Similar studies could provide valuable insights and introduce new approaches for theoretical and experimental investigations of the kinetics of droplet formation and thin-film growth. We have therefore undertaken the first step in this direction. This Letter is a brief report of our findings.

Cluster growth in vapor-deposition experiments is governed by two distinct mechanisms.[1] The first process is direct absorption from the vapor and the second is cluster-cluster aggregation. But in contrast to diffusion-limited cluster-cluster aggregation,[9] clusters aggregate when they contact,[10] rather than by migration and collision. As deposition and growth of clusters continues, the separation of various clusters decreases and—upon contact—clusters coalesce to form larger clusters. The geometry of the clusters depends on the state of the coalescing particles. When the substrate temperature is near or above the bulk melting point of the condensing material, clusters are liquid and spherical as a Fig. 1(a). *In situ* electron microscope observations[10] have confirmed that the fusion of two liquid droplets leads to the formation of a new spherical droplet with no loss in volume. It is this type of growth that we study in this Letter.

As a generalization of the growth of spherical droplets, we assume that when a droplet of radius r_1 joins to a droplet of radius r_2, a new droplet is formed, centered on the center of mass of the two original droplets, with a radius r which is given by

$$r=(r_1^D+r_2^D)^{1/D}, \tag{1}$$

where D can be considered as the *effective dimensionality* of the droplets. Note that, when the droplet dimension D is less than or equal to the dimension of the space d, $r \geq (r_1^D+r_2^D)^{1/d}$ so that after a finite time a single droplet forms which extends across the entire system. This phenomenon is similar to percolation[11] and gelation.[6,11] For $D>d$, $r<(r_1^D+r_2^D)^{1/d}$ and there is no gelation in a finite time and the growth proceeds much in the same manner as in low-density colloidal aggregation.[9] This implies that by using D as a variable parameter we can investigate a variety of interesting growth conditions, including percolation[11] and aggregation[9] of droplets. Since the experimental results in thin-film growth correspond to $D=3$ and $d=2$, in this Letter we will concentrate mainly on the case $D \geq d$.

In order to develop a description of the droplet-size distribution, in analogy with the scaling approach for aggregation processes,[7-9] we first assume that there exists only one characteristic cluster size in the system. Let $S(t)$ be the mean droplet size which is defined by

$$S(t)=\sum s^2 n_s(t) / \sum s n_s(t), \tag{2}$$

where $n_s(t)$ is the number of droplets of size s at time t. Since the mean droplet size increases with time, we assume thaat $S(t)$ and the mean droplet radius $R(t)$, which is defined by $R(t) \sim S(t)^{1/D}$, diverge as

$$S(t) \sim t^z \text{ and } R(t) \sim t^{z/D}, \tag{3}$$

where the dynamic exponent z must depend on both d and D. The total number of droplets in the system, $N(t)$, which is given by $N(t)=\sum n_s(t)$, is expected to decrease with an exponent z' as

$$N(t) \sim t^{-z'}. \tag{4}$$

We generalize the scaling description of the cluster-size distribution in aggregation processes,[7] and write

$$n_s(t) \sim s^{-\theta} f(s/S(t)). \tag{5}$$

The scaling function $f(x)$ has an interesting structure which is discussed later. Since the total mass in the system is not constant, the exponent θ depends on d and D and does not have a *superuniversal* value of 2 as in aggregation processes.[7] However, in the droplet-growth problem, the time t is equal to the total number of particles that have been added to the system. Using (3) and (5) we can write

$$\rho=t=\sum s n_s(t) \sim \int ds\, s^{1-\theta} f(s/S(t)) \sim S^{2-\theta} \int dx\, x^{1-\theta} f(x) \sim t^{z(2-\theta)}, \tag{6}$$

where ρ is the density of the system. Since the second integral on the right-hand side of (6) is independent of t, (6) implies that

$$\theta + 1/z = 2. \tag{7}$$

Therefore, $\theta \leq 2$, because $z>0$.

We now show how the exponents θ and z can be determined *exactly*. Let us define the correlation function $G(r)$ to be the probability that a site at distance r from an occupied site in a finite droplet is also occupied and belongs to the same droplet. In terms of $G(r)$, the mean cluster size $S(t)$ is given by

$$S(t)=\int d^d r\, G(r). \tag{8}$$

Since masses scale with $S(t)$, lengths are expected to scale with $R(t)$, i.e., $R(t)$ is the only length in the problem. Therefore, we assume that $G(r)$ can be written in the form

$$G(r)=\rho g(r/R), \tag{9}$$

where $g(x)$ is a scaling function which depends only on the ratio of r to mean cluster radius R. Inserting (9) in (8), and using (3) and (6), we find

$$S(t)=\rho R^d \int d^d x\, g(x) \sim t^{1+zd/D}. \tag{10}$$

In comparing (3) with (10), and using the exponent rela-

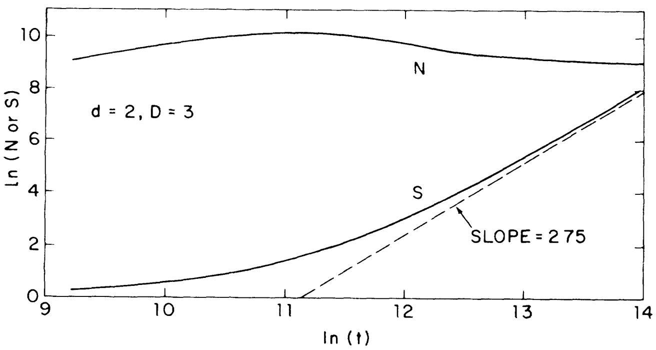

FIG. 2. The time dependence of the mean droplet size, $S(t)$, and the total number of droplets, $N(t)$, obtained by averaging 21 simulations.

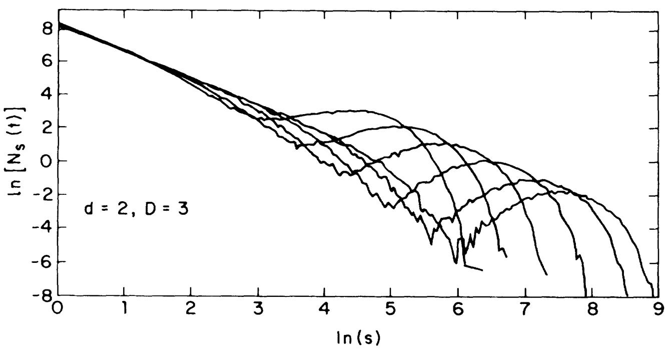

FIG. 3. The time-dependent droplet-size distribution at six stages during the same simulations as the data in Fig. 2. Asymptotically the droplet-size distribution has a bimodal structure with an initial power-law decay, superimposed on an approximately monodispersed, bell-shaped distribution peaked at the mean cluster size.

tion (7), we find

$$z = D/(D-d), \quad \theta = (D+d)/D \tag{11a}$$

and

$$n_s(t) \sim s^{-(1+d/D)} f(s/S(t)). \tag{11b}$$

To the best of our knowledge, these results have not been obtained previously. Note that, for $D=d$, $\theta=2$, $z \rightarrow \infty$, and $S(t)$ grows exponentially. Although we have the correct scaling form for n_s we cannot determine the exponent z' [Eq. (4)], because in contrast to (10) the dimensionless integral diverges in the lower limit.

We have developed a realistic, yet simple, model for the growth of the droplets. In our model, droplets of a fixed radius r_0 are added at random to a d-dimensional system of size L^d with periodic boundary conditions. Whenever two particles touch or overlap they are coalesced with mass conservation. The new droplet is centered on the center of mass of the two original droplets with a radius given by (1). If this droplet overlaps one or more other droplets, they are also coalesced and this procedure continues until no overlaps remain. A typical example, in which droplets with $D=3$ and a radius $r_0=0.75$ were added at random to a surface of size 256×256, is shown in Fig. 1(b), at time t when the mean cluster size has reached a mass of 1000 particles. Comparison of Figs. 1(a) and 1(b) shows that there are many similarities between the experimental data and our simulation. For example, the existence of depleted zones around large droplets is evident in both figures. These depleted regions are left behind by coalescence of two large droplets, before new particles have had a chance to accumulate there.

Figure 2 shows the time dependence of the mean droplet size, $S(t)$, measured in units of the mass of the added particles, and of the total number of droplets, $N(t)$. The data were obtained by averaging 21 simulations. The results are $z \approx 2.8$ and $z' \approx 0.27$. The value $z \approx 2.8$ is in agreement with $z=3$ obtained from (11), but indicates that the simulations are not yet in the asymptotic regime.

Figure 3 shows the time-dependent droplet-size distribution at six stages during the same simulations. These results indicate that asymptotically the droplet-size distribution has a novel structure with two distinctive features: an initial power-law decay, superimposed on an approximately monodispersed, bell-shaped distribution peaked at the mean cluster size. The existence of a bimodal distribution is different from those found in percolation,[6,11] which always has a power-law decay, and aggregation systems,[5,7-9] which have either a power-law decay or a bell-shaped form. The scaling of the droplet-size distribution for various times is clearly demonstrated in Fig. 4 where $s^\theta n_s(t)$ is plotted against $s/S(t)$ according to Eqs. (5) and (11). We have obtained similarly good scaling plots for other values of D in $d=1$, 2, and 3. In addition to θ, which we determine from the scaling plots, we have also determined the exponent τ which can be defined in the power-law–decay part of n_s by $n_s \sim s^{-\tau}$. The simulation data indicate that τ is equal to θ, implying that $f(x)$ goes to a constant for $x \ll 1$, and it

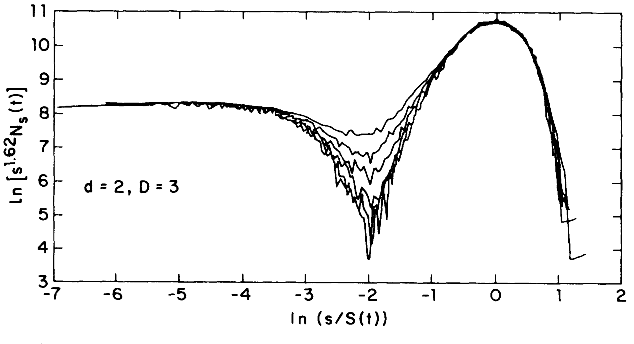

FIG. 4. The scaling of the cluster-size distributions shown in Fig. 3. We have obtained similarly good scaling plots for other values of D in $d=1$, 2, and 3.

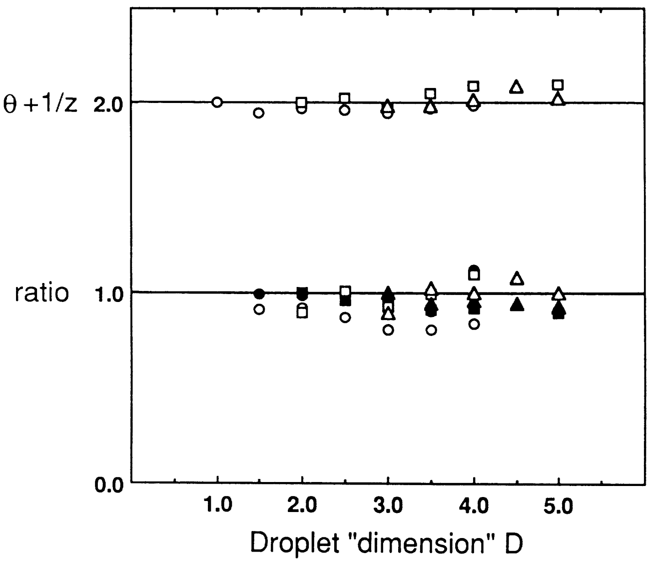

FIG. 5. The upper points are the simulation results for $\theta+1/z$, and the lower points are the ratios $z(D-d)/D$ (open symbols) and $\theta D/(d+D)$ (solid symbols) plotted against D for $d=1$ (circles), 2 (squares), and 3 (triangles).

has a bell-shaped form which peaks at $x=1$ and decays faster than any power of x for $x<1$ and $x>1$.

The results of the simulations are compared with the theoretical predictions (7) and (11) in Fig. 5, where the simulation results for $\theta+1/z$, $z(D-d)/D$, and $\theta D/(d+D)$ are plotted against D for $d=1$, 2, and 3. Within the accuracy of the simulations there is good agreement between theory and simulation. Any discrepancies can be attributed to the fact that the simulations have not yet reached the true asymptotic limit.

The form of the droplet-size distribution and its evolution to a bimodal shape, shown in Fig. 3, are in good agreement with the preliminary data recently obtained by Carr and Caldwell[12] for the droplet-size distribution of time droplets formed on the surface of a sapphire sample. Presently they[12] are carrying out detailed measurements and analysis of the droplet-size distribution in several different systems in order to make quantitative comparisons with the model and the theoretical predictions.

We can also make a qualitative comparison between our predictions and the experiment carried out by Beysens and Knobler[3] on the growth of breath figures, which are patterns that are formed when a vapor is condensed onto a cold surface. They measured the growth of $R(t)$ with time using light scattering and found that $R(t) \sim t^{0.75 \pm 0.05}$. Assuming spherical drops, we find $z=2.25 \pm 0.15$, in reasonable agreement with the value $z=3$ obtained from (11). The difference between the two results may be attributed to presence of gravity and evaporation, which are not included in our model.

In conclusion, we presented a scaling description of the droplet-size distribution for vapor-deposited thin films where a distribution of droplets is formed by nucleation, growth, and coalescence. Using general scaling arguments, the critical exponents describing the droplet-size distribution and the growth law for the mean droplet size were calculated exactly. We developed a simple and general droplet-growth model and demonstrated that asymptotically the droplet-size distribution has a bimodal structure which is in good agreement with measurements of the distribution of vapor-deposited tin droplets.[12] The simulation data are also in agreement with the theoretical predictions in $d=1$, 2, and 3. The scaling approach and the droplet-growth model presented here are effective methods for describing droplet-growth processes and we hope that this work will stimulate experimental and theoretical investigations of similar systems.

We would like to thank Larry Carr, Mehran Kardar, and Scott Anderson for useful conversations. One of us (P.M.) would like to acknowledge conversations with C. M. Knobler and Z.-Y. Chen which stimulated his interest in this problem. We would like to specially thank Larry Carr and Bryan Caldwell for sharing their data with us prior to publication. This work was supported by the U.S. Office of Naval Research and the Petroleum Research Fund Administered by the American Chemical Society.

---

[1] B. Lewis and J. C. Anderson, *Nucleation and Growth of Thin Films* (Academic, New York, 1978), and references therein.

[2] B. J. Mason, *The Physics of Clouds* (Oxford Univ. Press, London, 1957).

[3] D. Beysens and C. M. Knobler, Phys. Rev. Lett. **57**, 1433 (1986).

[4] J. D. Gunton, M. San Miguel, and P. S. Sahni, in *Phase Transitions and Critical Phenomena,* edited by C. Domb and J. L. Lebowitz (Academic, London, 1983), Vol. 8.

[5] S. K. Friedlander, *Smoke, Dust and Haze: Fundamentals of Aerosol Behavior* (Wiley, New York, 1977).

[6] R. M. Ziff, E. M. Hendriks, and M. H. Ernst, Phys. Rev. Lett. **49**, 593 (1982).

[7] T. Vicsek and F. Family, Phys. Rev. Lett. **52**, 1669 (1984).

[8] F. Family, P. Meakin, and J. M. Deutch, Phys. Rev. Lett. **57**, 727 (1986).

[9] P. Meakin, in *Phase Transitions and Critical Phenomena,* edited by C. Domb and J. L. Lebowitz (Academic, London, 1988), Vol. 12.

[10] M. J. Stowell, T. J. Law, and J. Shaw, Proc. Roy. Soc. London A **318**, 231 (1970).

[11] D. Stauffer, *Introduction to Percolation Theory* (Taylor & Francis, London, 1985).

[12] G. L. Carr and B. Caldwell, private communications, and unpublished.

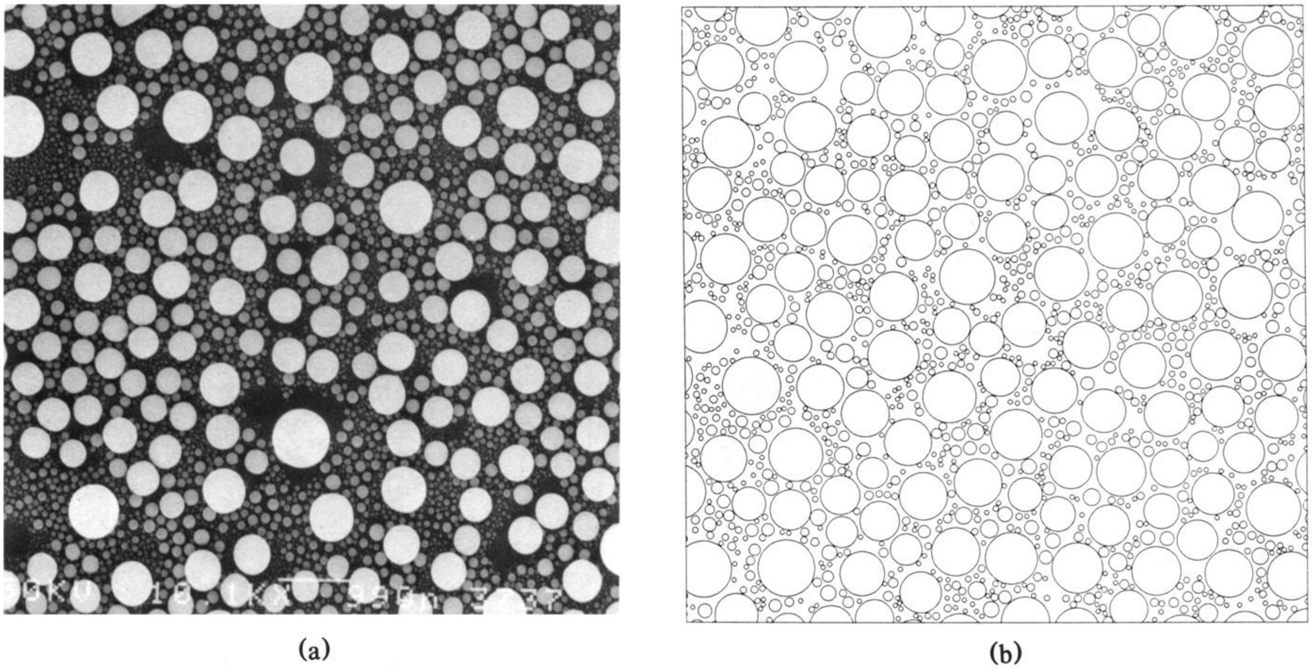

FIG. 1. (a) An electron micrograph of vapor-deposited tin on the surface of a sapphire sample held at 230 °C. The uniform size of the larger droplets indicates that there exists an approximately monodispersed distribution of droplets which is superimposed on wide distribution of smaller droplets. (b) A typical example from the simulation in which spherical droplets with a radius $r_0 = 0.75$ were added at random to a surface of size 256×256. Depleted zones around large droplets are evident in both figures.